

From randomized benchmarking experiments to gate-set circuit fidelity: how to interpret randomized benchmarking decay parameters

Arnaud Carignan-Dugas,^{1,*} Kristine Boone,¹ Joel J. Wallman,¹ and Joseph Emerson^{1,2}

¹*Institute for Quantum Computing and the Department of Applied Mathematics,
University of Waterloo, Waterloo, Ontario N2L 3G1, Canada*

²*Canadian Institute for Advanced Research, Toronto, Ontario M5G 1Z8, Canada*
(Dated: September 11, 2018)

Randomized benchmarking (RB) protocols have become an essential tool for providing a meaningful partial characterization of experimental quantum operations. While the RB decay rate is known to enable estimates of the average fidelity of those operations under gate-independent Markovian noise, under gate-dependent noise this rate is more difficult to interpret rigorously. In this paper, we prove that single-qubit RB decay parameter p coincides with the decay parameter of the *gate-set circuit fidelity*, a novel figure of merit which characterizes the expected average fidelity over arbitrary circuits of operations from the gate-set. We also prove that, in the limit of high-fidelity single-qubit experiments, the possible alarming disconnect between the average gate fidelity and RB experimental results is simply explained by a basis mismatch between the gates and the state-preparation and measurement procedures, that is, to a unitary degree of freedom in labeling the Pauli matrices. Based on numerical evidence and physically motivated arguments, we conjecture that these results also hold for higher dimensions.

I. INTRODUCTION

The operational richness of quantum mechanics hints at an unprecedented computational power. However, this very richness carries over to a vast range of possible quantum error processes for which a full characterization is impractical for even a handful of quantum bits (qubits). Randomized benchmarking (RB) experiments [1–8] were introduced to provide a robust, efficient, scalable, SPAM-independent¹, partial characterization of specific sets of quantum operations of interest, referred to as gate-sets. Such experiments have been widely adopted across all platforms for quantum computing, eg. [9–17], and have become a critical tool for characterizing and improving the design and control of quantum bits (qubits).

Recently it has been shown that RB experiments on an arbitrarily large number of qubits will always produce an exponential decay under arbitrary Markovian error models (that is, where errors are represented as completely-positive maps). This ensures a well-defined theoretical characterization of these experiments and enables an important test for the presence of non-Markovian errors, in spite of the gauge freedom between the experimental quantities and a theoretical figure of merit such as the average gate fidelity [18–20]. However, this theoretical advance still lacks a clear physical interpretation that rigorously connects the experimentally observed decay to a fidelity-based characterization of a physical set of gate-dependent errors. Linking an experimentally measured quantity to a physically meaningful figure of merit is not a mere intellectual satisfaction. It is crucial to ensure that a quantity measured in the context of a process characterization protocol indeed yields an outcome

that assesses the quality of operations. What if a very noisy quantum device could yield a decent RB parameter? What if there exist scenarios where RB substantially underestimates the quality of a quantum device?

In this paper, we show that in the regime of high fidelity gates on single qubits, a simple physical interpretation of RB data does exist and allows a reliable characterization of quantum operations. Further we conjecture, based on numerical evidence, that such an interpretation extends to arbitrary dimensions. Consequently, this work provides the theoretical foundation behind a fundamental tool for identifying and eliminating errors through examining the results of RB experiments.

Consider a targeted ideal gate-set $\mathbb{G} = \{\mathcal{G}\}$ and its noisy implementation $\tilde{\mathbb{G}} = \{\tilde{\mathcal{G}}\}$. We denote a circuit composed of m elements by

$$\tilde{\mathcal{G}}_{m:1} := \tilde{\mathcal{G}}_m \cdots \tilde{\mathcal{G}}_2 \tilde{\mathcal{G}}_1. \quad (1)$$

For leakage-free RB experiments with arbitrarily gate-dependent (but still Markovian) errors, the average probability of an outcome μ after preparing a state ρ and applying a circuit of $m + 1$ operations that multiply to the identity is [19, 20]

$$\mathbb{E}_{\mathcal{G}_{m+1:1}} \langle \mu, \tilde{\mathcal{G}}_{m+1:1}(\rho) \rangle = Ap^m + B + \epsilon(m), \quad (2)$$

where $\langle M_1, M_2 \rangle := \text{Tr} M_1^\dagger M_2$ refers to the Hilbert-Schmidt inner product. On the right-hand side of eq. (2), A and B are independent of m (i.e., they only depend upon ρ , μ and $\tilde{\mathcal{G}}$) and $\epsilon(m)$ is a perturbative term that decays exponentially in m .

By design, RB gives some information about the error rate of motion-reversal (i.e., identity) circuits composed of gate-set elements. In this paper, we show how this information relates to general circuits. Consider the traditional notion of *average fidelity* for a noisy circuit $\tilde{\mathcal{C}}$ to

* arnaud.carignan@gmail.com

¹ SPAM stands for “State preparation and measurement”.

a target unitary circuit \mathcal{C} ,

$$F(\tilde{\mathcal{C}}, \mathcal{C}) := \int \langle \tilde{\mathcal{C}}(\psi), \mathcal{C}(\psi) \rangle d\psi, \quad (3)$$

where the integral is taken uniformly over all pure states. Equation (3) corresponds to the definition of the usual notion of *average gate fidelity*, but is instead formulated in terms of “circuit”, which is to be understood as a sequence of elementary gates. We introduce this nuance to define a novel figure of merit, the *gate-set circuit fidelity*, which compares all possible sequences of m implemented operations from the gate-set $\tilde{\mathbb{G}}$ to their targets in \mathbb{G} ,

Definition 1 (*gate-set circuit fidelity*).

$$\mathcal{F}(\tilde{\mathbb{G}}, \mathbb{G}, m) := \mathbb{E} \left[F(\tilde{\mathcal{G}}_{m:1}, \mathcal{G}_{m:1}) \right]. \quad (4)$$

The case $m = 1$ yields the average fidelity of the gate-set $\tilde{\mathbb{G}}$ to \mathbb{G} . In general, the overall action of ideal circuits $\mathcal{G}_{m:1}$ is reproduced by $\tilde{\mathcal{G}}_{m:1}$ with fidelity $\mathcal{F}(\tilde{\mathbb{G}}, \mathbb{G}, m)$. Having access to the gate-set circuit fidelity enables going beyond quantifying the quality of gate-set elements as it also quantifies the quality of circuits based on those elements. In this paper, we prove that for all single-qubit gate-sets with fidelities close to 1 and for an appropriately chosen targeted gate-set \mathbb{G} , the gate-set circuit fidelity can be closely estimated via RB experiments, for all circuit lengths m , even in cases of highly gate-dependent noise models. This is possible because it turns out that $\mathcal{F}(\tilde{\mathbb{G}}, \mathbb{G}, m)$ essentially behaves like an exponential decay in m , uniquely parametrized by the RB decay constant p . The robust inclusion of gate-dependence is a major step forward since it encompasses very realistic noise models. We conjecture this result to hold for higher dimensions, based on numerical evidences and physically motivated arguments. Notice that the gate-set circuit fidelity quantifies the expected fidelity of *all* circuits (built from gate-set elements), and not only motion-reversal ones. This is an important observation to keep in mind because although RB experiments intrinsically revolve around motion-reversal circuits, the figure of merit that it yields isn’t limited to such paradigm. Quantifying the quality of all circuits is much more useful than quantifying identity ones.

II. THE DYNAMICS OF THE GATE-SET CIRCUIT FIDELITY

It follows from the RB literature [1, 5] that for gate-independent noise models of the form $\tilde{\mathbb{G}} = \mathcal{E}\mathbb{G}$ or $\tilde{\mathbb{G}} = \mathbb{G}\mathcal{E}$, where \mathcal{E} is a fixed error, the gate-set circuit fidelity behaves exactly as

$$\mathcal{F}(\tilde{\mathbb{G}}, \mathbb{G}, m) = \frac{1}{d} + \frac{d-1}{d} p^m, \quad (5)$$

where p is estimated through standard RB by fitting to eq. (2) with $\epsilon(m) = 0$ and d is the dimension of the

system. The relationship between the survival probability decay curve and the decay in eq. (5) shouldn’t be surprising. Indeed, consider a RB experiment with a noise model of the form $\mathcal{E}\mathbb{G}$ and a perfect inversion step $\mathcal{G}_{m+1} \in \mathbb{G}$ and perfect SPAM. In such case, the gate-set circuit fidelity and the survival probability exactly coincide. A less trivial matter is to show the link between the RB decay parameter and eq. (5) for gate-dependent leakage-free noise models for which the choice of targeted gate-set is to be treated more carefully. In fact, as we will show, a poor choice of targeted gate-set can lead to a strong violation of eq. (5) in the sense that $1 - \mathcal{F}(\tilde{\mathbb{G}}, \mathbb{G}, m)$ can relatively differ from $1 - (\frac{1}{d} + \frac{d-1}{d} p^m)$ by multiple orders of magnitude. An appropriate choice of targeted gate-set will essentially restore the decay relation shown in eq. (5).

Equation (5) generalizes to

$$\mathcal{F}(\tilde{\mathbb{G}}, \mathbb{G}, m) = \frac{1}{d} + \frac{d-1}{d} f_{\text{tr}}(\tilde{\mathbb{G}}, \mathbb{G}, m), \quad (6)$$

where the fidelity on the traceless hyperplane is similar to the gate-set circuit fidelity, but is averaged over the traceless part of the pure states, $\psi_{\text{tr}} = \psi - \mathbb{I}/d$:

$$f_{\text{tr}}(\tilde{\mathbb{G}}, \mathbb{G}, m) := \frac{\mathbb{E} \left(\int \langle \tilde{\mathcal{G}}_{m:1}(\psi_{\text{tr}}), \mathcal{G}_{m:1}(\psi_{\text{tr}}) \rangle d\psi \right)}{\int \langle \psi_{\text{tr}}, \psi_{\text{tr}} \rangle d\psi}. \quad (7)$$

The integrand in the numerator of the right-hand side of eq. (7) can be visualized as the fidelity restricted on the Bloch space, comparing the ideally mapped Bloch vectors $\psi_{\text{tr}} \rightarrow \mathcal{G}_{m:1}(\psi_{\text{tr}})$ to their noisy analog $\tilde{\mathcal{G}}_{m:1}(\psi_{\text{tr}})$. Equation (6) is quickly obtained by realizing that the symmetric integral over the Bloch space $\int \psi_{\text{tr}} d\psi = 0$.

Under gate-dependent noise, $1 - f_{\text{tr}}(\tilde{\mathbb{G}}, \mathbb{G}, 1)$ could relatively differ from $1 - p$ by several orders of magnitude [18, 21]. Such discrepancy was seen as a serious concern: the observed RB decay seemingly fails in characterizing the quality of quantum operations. To see the possible immense disconnect between p and $f_{\text{tr}}(\tilde{\mathbb{G}}, \mathbb{G}, 1)$, consider the canonical example where single-qubit gates are perfectly implemented, but differ from the targets $\mathcal{G} \in \mathbb{G}$ by a labeling of the Pauli axes:

$$\tilde{\mathcal{G}}(X) = \mathcal{G}(Y), \quad (8a)$$

$$\tilde{\mathcal{G}}(Y) = \mathcal{G}(Z), \quad (8b)$$

$$\tilde{\mathcal{G}}(Z) = \mathcal{G}(X). \quad (8c)$$

This noise model would lead to an absence of decay in the survival probability, that is $p = 1$. Indeed, motion-reversal circuits are perfectly implementing the identity gate, regardless of the length of the circuit. A quick calculation results in $f_{\text{tr}}(\tilde{\mathbb{G}}, \mathbb{G}, m) = 0$, which demonstrates a difference in orders of magnitude $|\log(1 - p) - \log(1 - f_{\text{tr}}(\tilde{\mathbb{G}}, \mathbb{G}, 1))|$ that tends to infinity as $p \rightarrow 1$. The RB experiment indicates no operational error while the average gate fidelity indicates 1/2. Does the outcome of RB massively underestimate the

error? Notice that since the implementation error is a permutation of labels, there is actually no observable error in the device. The alarmingly low value of gate-set circuit fidelity of $\tilde{\mathbb{G}}$ to \mathbb{G} is simply a consequence of a poor choice of targeted gate-set.

As a more involved example, let the noise model be $\tilde{\mathbb{G}} = \mathcal{U}\mathbb{G}\mathcal{U}^\dagger$ for any non-identity unitary channel \mathcal{U} and let the set of targeted operations be \mathbb{G} (this includes our previous mislabeling example as a special scenario). In such cases $f_{\text{tr}}(\tilde{\mathbb{G}}, \mathbb{G}, 1)$ can take any value in the interval $[0, 1)$, depending on the choice of \mathcal{U} . However, using the same argument as in the previous example, the survival probability is not subject to a decay ($p = 1$), showing once again how the decay parameter could arbitrarily differ from a poorly defined average gate fidelity. This apparent disconnect arises due to a *basis mismatch* between the bases in which the noisy gate-set and the targeted gate-set are defined. A reconciliation of the RB observations with a gate-set circuit fidelity is obtained by changing the set of targets to $\mathcal{U}\mathbb{G}\mathcal{U}^\dagger$ since $f_{\text{tr}}(\tilde{\mathbb{G}}, \mathcal{U}\mathbb{G}\mathcal{U}^\dagger, 1) = 1$. One might argue that implementing $\tilde{\mathbb{G}} = \mathcal{U}\mathbb{G}\mathcal{U}^\dagger$ instead of the ideal \mathbb{G} should raise an operational error. Not necessarily: consider a circuit uniquely constructed from operations $\tilde{\mathcal{G}}_i \in \tilde{\mathbb{G}}$. According to Born's rule, the probability of measuring the outcome i associated with the positive operator μ_i after performing the circuit on a state ρ is:

$$\begin{aligned} p_i &= \langle \mu_i, \tilde{\mathcal{G}}_{m:1}(\rho) \rangle \\ &= \langle \mu_i, \mathcal{U}\mathcal{G}_m\mathcal{U}^\dagger \cdots \mathcal{U}\mathcal{G}_2\mathcal{U}^\dagger\mathcal{U}\mathcal{G}_1\mathcal{U}^\dagger(\rho) \rangle \\ &= \langle \mu_i, \mathcal{U}\mathcal{G}_{m:1}\mathcal{U}^\dagger(\rho) \rangle \\ &= \langle \mu'_i, \mathcal{G}_{m:1}(\rho') \rangle, \end{aligned} \quad (9)$$

where $\rho' = \mathcal{U}^\dagger(\rho)$, $\mu'_i = \mathcal{U}^\dagger(\mu_i)$. That is, the error can be interpreted as part of SPAM procedures instead of operations. Since the unitary transformation can be pushed to either SPAM procedures or coherent manipulations, it should be seen as a mismatch between them. Indeed, the physical unitary conjugation $\tilde{\mathbb{G}} = \mathcal{U}\mathbb{G}\mathcal{U}^\dagger$ doesn't affect the *internal action* of operations, but exclusively the connection between operations and SPAM procedures. Changing the targeted gate-set \mathbb{G} to $\mathcal{U}\mathbb{G}\mathcal{U}^\dagger$ is allowed by the degree of freedom in labeling what is the basis for SPAM procedures and what is the basis for processes.

In appendix A, we show how exactly the disconnect between p^m and $f_{\text{tr}}(\tilde{\mathbb{G}}, \mathcal{U}\mathbb{G}\mathcal{U}^\dagger, m)$ depends on the choice of targeted gate-set $\mathcal{U}\mathbb{G}\mathcal{U}^\dagger$. That is, we provide an expression of the form

$$f_{\text{tr}}(\tilde{\mathbb{G}}, \mathcal{U}\mathbb{G}\mathcal{U}^\dagger, m) = C(\mathcal{U})p^m + D(m, \mathcal{U}), \quad (10)$$

where \mathcal{U} is a physical unitary channel (see theorem 5). A first interesting observation is that $D(m, \mathcal{U})$ is typically negligible or becomes rapidly negligible as it is also expo-

entially suppressed in m^2 . This means that the relative variation in f_{tr} as the circuit grows in length,

$$\frac{f_{\text{tr}}(\tilde{\mathbb{G}}, \mathcal{U}\mathbb{G}\mathcal{U}^\dagger, m+1)}{f_{\text{tr}}(\tilde{\mathbb{G}}, \mathcal{U}\mathbb{G}\mathcal{U}^\dagger, m)} = p + \delta(m, \mathcal{U}), \quad (11)$$

depends weakly on the choice of targeted gate-set. More precisely, $\delta(m, \mathcal{U})$ is composed of two factors: the first one decays exponentially in m and is at most of order $(1-p)^{m/2}$, while the second carries the dependence in \mathcal{U} ; the existence of a specific choice of \mathcal{U} such that this last factor becomes at most of order $(1-p)^{3/2}$ is proven in the single-qubit case (appendix B), and conjectured to hold in general. The explicit behaviour of $\delta(m, \mathcal{U})$ given a numerically simulated gate-dependent noise model is illustrated in fig. 1.

Consequently, the gate-set circuit fidelity can be updated with a good approximation through the recursion relation

$$\mathcal{F}(\tilde{\mathbb{G}}, \mathcal{U}\mathbb{G}\mathcal{U}^\dagger, m+1) \approx \frac{1}{d} + p \left(\mathcal{F}(\tilde{\mathbb{G}}, \mathcal{U}\mathbb{G}\mathcal{U}^\dagger, m) - \frac{1}{d} \right). \quad (12)$$

Roughly speaking, this means that the choice of basis \mathcal{U} in which are expressed the targets in $\mathcal{U}\mathbb{G}\mathcal{U}^\dagger$ is not highly significant when it comes to updating the gate-set circuit fidelity as the circuit grows in depth. The RB decay rate p enables the decrease in fidelity due to adding a gate to a circuit to be predicted.

However, to provide insight on the total value of the gate-set circuit fidelity given a circuit's length m , we need a stronger relation between the RB estimate of p and the gate-set circuit fidelity. Fortunately, the basis freedom in the choice of targeted gate-set can be fixed in a way that allows us to estimate the total change in gate-set circuit fidelity for arbitrary circuit's lengths.

In appendix B, we prove that the potentially large disconnect between p and $f_{\text{tr}}(\tilde{\mathbb{G}}, \mathcal{U}\mathbb{G}\mathcal{U}^\dagger, 1)$ under general gate-dependent noise is almost completely accounted for by a basis mismatch which, as we argued earlier, doesn't exactly correspond to a process error since unitary conjugation does not affect the internal dynamics of operations.

Proposition 2. *For any single-qubit noisy gate-set $\tilde{\mathbb{G}}$ perturbed from \mathbb{G} , there exists an ideal targeted gate-set $\mathcal{U}\mathbb{G}\mathcal{U}^\dagger$, where \mathcal{U} is a physical unitary, such that*

$$\mathcal{F}(\tilde{\mathbb{G}}, \mathcal{U}\mathbb{G}\mathcal{U}^\dagger, m) = \frac{1}{d} + \frac{d-1}{d}p^m + O((1-p)^2). \quad (13)$$

In fact, we conjecture this result to hold for any dimension, or at least for most realistic gate-dependent noise models. To grasp the physical reasoning behind this, we

² Since $D(1, \mathcal{U})$ is typically close to 0, the exponential suppression is quite effective compared to $p^m \approx 1 - m(1-p)$ which is essentially linear for small m .

refer to the end of appendix B, as it rests on some prior technical analysis. The extension of proposition 2 to 2-qubit systems is supported by numerical evidences (see appendices A to B).

The unitary freedom appearing in the gate-set circuit fidelity means that there exists an infinite amount of fidelity-based figures of merit describing noisy circuits, one for each infinitely many targeted gate-set \mathcal{UGU}^\dagger . Of course, there exist choices of targeted operations that yield in gate-set circuit fidelities that differ from eq. (13) (see [18, 21]); the example shown in eqs. (8a) to (8c) is an elementary instance thereof. Proposition 2 simply states that there exists a natural choice of gate-set \mathcal{UGU}^\dagger that allows connecting the outcome of an RB experiment to a gate-set circuit fidelity. The choice of basis \mathcal{U} is like taking the perspective of the gates rather than the perspective of SPAM procedures (as is implicitly done when defining gates relative to the energy eigenbasis of the system). In this picture, the gate-set circuit fidelity describes the accuracy of the internal behaviour of operations as they act in concert.

To reformulate the result, the family of circuits $\tilde{\mathcal{G}}_{m:1}$ built from a composition of m noisy operations $\tilde{\mathcal{G}} \in \tilde{\mathbb{G}}$ mimics the family of ideal circuits $\mathcal{UG}_{m:1}\mathcal{U}^\dagger$ with fidelity $\frac{1}{d} + \frac{d-1}{d}p^m$. In the paradigm where the initially targeted operations $\mathcal{G} \in \mathbb{G}$ are defined with respect to SPAM procedures, \mathcal{U} captures the misalignment between the basis in which the operations $\tilde{\mathcal{G}} \in \tilde{\mathbb{G}}$ are defined and the basis defined by SPAM procedures. This goes farther: consider an additional gate-set, for which the targeted operations $\mathcal{H} \in \mathbb{H}$ are also defined respect to SPAM procedures. From proposition 2, there exists a physical unitary \mathcal{V} for which $\tilde{\mathcal{H}}_{m:1}$ imitates the action of $\mathcal{V}\mathcal{H}_{m:1}\mathcal{V}^\dagger$ with fidelity $\frac{1}{d} + \frac{d-1}{d}q^m$ (where q is estimated through RB). $\mathcal{U}^\dagger\mathcal{V}$ captures the basis mismatch between the gate-sets $\tilde{\mathbb{G}}$ and $\tilde{\mathbb{H}}$. Such a non-trivial mismatch could easily be imagined if, for instance, gates belonging to $\tilde{\mathbb{H}}$ were obtained through a different physical process than $\tilde{\mathbb{G}}$, or calibrated with regards to alternate points of reference.

III. FINDING THE APPROPRIATE SET OF TARGETED GATES FOR SPECIFIC NOISE MODELS

We now discuss how the appropriate unitary conjugation on the initial targeted gate-set can be calculated for specific noise models, whether from numerical simulations, analytic approximations, or tomographic reconstructions. As shown in theorem 5 and eq. (10), the total change of gate-set circuit fidelity depends on the physical basis in which the ideal gate-set is expressed. In the single-qubit case, we showed the existence of a physical basis \mathcal{U} that reconciles $f_{\text{tr}}(\tilde{\mathbb{G}}, \mathcal{UGU}^\dagger, m)$ with p^m through proposition 2. One might suspect that the unitary \mathcal{U} can be found through the maximization of the gate-set

fidelity:

$$\mathcal{U} = \underset{\mathcal{V}}{\text{argmax}} \mathcal{F}(\tilde{\mathbb{G}}, \mathcal{V}\mathbb{G}\mathcal{V}^\dagger, 1), \quad (14)$$

and indeed this would handle noise models of the form $\tilde{\mathbb{G}} = \mathcal{U}\mathcal{E}\mathbb{G}\mathcal{U}^\dagger$, as

$$p = f_{\text{tr}}(\tilde{\mathbb{G}}, \mathcal{UGU}^\dagger, 1) \geq f_{\text{tr}}(\tilde{\mathbb{G}}, \mathbb{G}, 1).$$

However, this hypothesis fails for simple noise models of the form $\tilde{\mathbb{G}} = \mathcal{U}^\dagger\mathcal{E}\mathbb{G}\mathcal{U}^\dagger$, where

$$p = f_{\text{tr}}(\tilde{\mathbb{G}}, \mathcal{UGU}^\dagger, 1) \leq f_{\text{tr}}(\tilde{\mathbb{G}}, \mathbb{G}, 1).$$

Those last two examples show that p can be greater or less than $f_{\text{tr}}(\tilde{\mathbb{G}}, \mathbb{G}, 1)$, depending on the noise model. More examples are derived in [18, 21]. This particular case study is informative as these two last noise models share something in common: there exists a choice of unitary \mathcal{U} that cancels the noisy map on the right of the noisy gate-set. Although such exact cancellation is not always possible, we now show that a close approximation is sufficient. Consider the slightly more general noise model of the form $\tilde{\mathbb{G}} = \mathcal{E}_L\mathbb{G}\mathcal{E}_R$, where we allow fixed but arbitrary error maps to the left and the right of an ideal gate-set. It can be shown while staying under the scope of the original analysis provided in [5, 6] that $p^m = f_{\text{tr}}(\mathcal{E}_R\mathcal{E}_L\mathbb{G}, \mathbb{G}, m)$, since $\mathcal{E}_R\mathcal{E}_L$ is the effective error map between two otherwise perfect implementations of the gate-set elements. In the single-qubit case (and for many, if not all physically motivated higher dimensional noise models) there exists a unitary operation \mathcal{U} such that

$$F(\mathcal{E}_R\mathcal{E}_L, \mathcal{I}) = \mathcal{F}(\mathcal{E}_L\mathbb{G}\mathcal{E}_R, \mathcal{UGU}^\dagger, 1) + O((1-p)^2), \quad (15)$$

(see appendix B). That is, the fidelity of the map between two noisy gate-sets can be seen as the gate-set circuit fidelity between a noisy gate-set and an appropriately targeted ideal one. A choice of such physical unitary is

$$\mathcal{U} = \underset{\mathcal{V}}{\text{argmax}} F(\mathcal{E}_R\mathcal{V}, \mathcal{I}), \quad (16)$$

which essentially cancels the unitary part of \mathcal{E}_R ³. Another way to see this is that the unitary freedom allows us to reexpress the errors \mathcal{E}_L , \mathcal{E}_R as

$$\begin{aligned} \mathcal{E}_L &\rightarrow \mathcal{U}^\dagger\mathcal{E}_L \\ \mathcal{E}_R &\rightarrow \mathcal{E}_R\mathcal{U}. \end{aligned}$$

We can then chose the unitary that depletes $\mathcal{E}_R\mathcal{U}$ from any coherent component. Intuitively, reexpressing the error on one side to make it incoherent prevents any type of unitary conjugation of the form $\tilde{\mathbb{G}} = \mathcal{U}\mathcal{E}\mathbb{G}\mathcal{U}^\dagger$.

³ Of course, $\underset{\mathcal{V}}{\text{argmax}} F(\mathcal{V}^\dagger\mathcal{E}_L, \mathcal{I})$ would also fulfill eq. (15).

For more general gate-dependent noise models, the idea remains more or less the same. As shown in appendix B, the right error \mathcal{E}_R is replaced by its generalization, the 4th order right error $\mathcal{E}_R^{(4)} = \mathbb{E} \left[\mathcal{G}_{4:1}^\dagger \tilde{\mathcal{G}}_{4:1} \right]$ (eq. (B4a)). From there, we find:

Proposition 3 (Finding the appropriate targeted gate-set). *A proper choice of physical basis \mathcal{U} for which eq. (13) applies is*

$$\mathcal{U} = \underset{\mathcal{V}}{\operatorname{argmax}} F \left(\mathbb{E} \left[\mathcal{G}_{4:1}^\dagger \tilde{\mathcal{G}}_{4:1} \right] \mathcal{V}, \mathcal{I} \right), \quad (17)$$

\mathcal{U} cancels the unitary part of the 4th order right error.

This provides a means to guide the search of the appropriate ideal targeted gate-set of comparison $\mathcal{U}\mathbb{G}\mathcal{U}^\dagger$ given a numerical noise model $\tilde{\mathbb{G}}$. Indeed, the 4th order right error is easily found, either by direct computation of the average $\mathbb{E} \left[\mathcal{G}_{4:1}^\dagger \tilde{\mathcal{G}}_{4:1} \right]$, or more efficiently by solving the eigensystem defined in eq. (A7a). The optimization defined in eq. (17) can be solved via a gradient ascent parametrized over the $d^2 - 1$ degrees of freedom of $SU(d)$.

In the single-qubit case, the optimization procedure can be replaced by an analytical search. Given the process matrix $\mathcal{E}_R^{(4)}$ of the 4th order right error, it suffices to find the polar decomposition of its 3×3 submatrix acting on the Bloch vectors: $\mathcal{E}_R^{(4)} \mathbf{\Pi}_{\text{tr}} = \mathcal{D}_{\text{tr}} \mathcal{V}_{\text{tr}}$. The unitary factor \mathcal{V} corresponds to \mathcal{U}^\dagger , while the positive factor \mathcal{D} captures an incoherent process (rigorously defined in eq. (B7)).

With this at hand, we performed numerically simulated RB experiments under gate-dependent noise models. Each of the 24 Cliffords was constructed by a sequence of X and Y pulses, $G_x = P(\sigma_x, \pi/2)$ and $G_y = P(\sigma_y, \pi/2)$, where

$$P(H, \theta) := e^{i\theta H/2}. \quad (18)$$

The 2-qubit Cliffords were obtained through the construction shown in [10, 12], where the 11520 gates are composed of single-qubit Clifford and CZ gates. The implementation of the 2-qubit entangling operation was consistently performed with an over-rotation: $\tilde{\mathcal{G}}_{CZ} = \mathcal{P}(\sigma_z^1 \sigma_z^2 - \sigma_z^1 - \sigma_z^2, \pi/2 + 10^{-1})$. In fig. 2, the single-qubit gate generators are modeled with a slight over-rotation: $\tilde{\mathcal{G}}_x = \mathcal{P}(\sigma_x, \pi/2 + 10^{-1})$ and $\tilde{\mathcal{G}}_y = \mathcal{P}(\sigma_y, \pi/2 + 10^{-1})$. This model exemplifies the failure of the maximization hypothesis proposed in eq. (14). In figs. 1 and 3, the single-qubit gate generators are followed by a short Z pulse, $\tilde{\mathcal{G}}_x = \mathcal{P}(\sigma_z, \theta_z) \mathcal{G}_x$ and $\tilde{\mathcal{G}}_y = \mathcal{P}(\sigma_z, \theta_z) \mathcal{G}_y$, which reproduces the toy model used in [18].

IV. CONCLUSION

RB experiments estimate the survival probability decay parameter p of motion-reversal circuits constituted of

operations from a noisy gate-set $\tilde{\mathbb{G}}$ of increasing length (see eq. (2)). While motion-reversal is intrinsic to the experimental RB procedure, the estimated decay constant p can be interpreted beyond this paradigm. In this paper we have shown that, in a physically relevant limit, the very same parameter determines an interesting figure of merit, namely the gate-set circuit fidelity (defined in eq. (4)): as a random operation from $\tilde{\mathbb{G}}$ is introduced to a random circuit constructed from elements in $\tilde{\mathbb{G}}$, p captures the expected relative change in the gate-set circuit fidelity through eq. (12).

It is also possible to characterize the full evolution of gate-set circuit fidelity as a function of the circuit length. In this paper, we have also demonstrated that given a single-qubit noisy gate-set $\tilde{\mathbb{G}}$ perturbed from \mathbb{G} , there exists an alternate set of targeted gates obtained through a physical basis change $\mathcal{U}\mathbb{G}\mathcal{U}^\dagger$ such that the gate-set circuit fidelity takes the simple form given in eq. (13). This gives a rigorous underpinning to previous work that has assumed that the experimental RB decay parameter robustly determines a relevant average gate fidelity (eq. (3)) for experimental control under generic gate-dependent scenarios. We conjecture a similar result to hold for higher dimensions and provide numerical evidence and physically motivated arguments to support this conjecture. Given any specific numerical noise model $\tilde{\mathbb{G}}$ perturbed from \mathbb{G} , we showed how to obtain a physical unitary \mathcal{U} for which eq. (13) holds. The procedure can be seen as a fidelity maximization of the 4th order right error acting on the gate-set through a unitary correction (see proposition 3).

The introduction of such a physical basis adjustment is natural because it has no effect on how errors accumulate as a function of the sequence length. Rather, it only reflects a basis mismatch to the experimental SPAM procedures. This is in principle detectable by RB experiments but in practice not part of the goals of such diagnostic experiments. In particular, differences in the (independent) basis adjustments required for distinct gate-sets will not appear in any characterization of the individual gate-sets, but will be detected when comparing RB experiments for this distinct gate-sets (e.g., comparing dihedral benchmarking and standard randomized benchmarking experiments which have distinct gate-sets but share gates in common, or comparing independent single-qubit RB on two qubits - which has no two-qubit entangling gate - with standard two-qubit RB). We leave the problem of characterizing relative basis mismatch between independent gate-sets as a subject for further work.

Appendix A: An expression for the total change in the gate-set circuit fidelity

In this section, we extend the standard RB analysis under gate-dependent noise provided in [19, 20] in order to prove the claim from eq. (11) that standard RB returns the relative variation of the gate-set circuit fidelity.

Let \mathcal{A} be the Liouville matrix of a linear map \mathcal{A} and $\Pi_{\text{tr}}(\rho) = \rho - \mathbb{1} \text{Tr} \rho / d$ be the projector onto the traceless component. We denote the Frobenius norm, which is defined by the Hilbert-Schmidt inner product, as $\|\cdot\|_F$. For instance, in the qubit case $\|\Pi_{\text{tr}}\|_F^2 = 3$. We denote the induced 2-norm as $\|\cdot\|_2$, which corresponds to the maximal singular value. Let e_j be the canonical unit vectors, $A = \sum_{j,k} a_{j,k} e_j e_k^T$, and

$$\text{vec}(A) = \sum_{j,k} a_{j,k} e_k \otimes e_j . \quad (\text{A1})$$

Using the identity

$$\text{vec}(ABC) = (C^T \otimes A) \text{vec}(B) , \quad (\text{A2})$$

we have

$$\begin{aligned} f_{\text{tr}}(\tilde{\mathbb{G}}, \mathbb{G}, m) &= \mathbb{E} \left(\frac{\langle \tilde{\mathcal{G}}_{m:1} \Pi_{\text{tr}}, \mathcal{G}_{m:1} \Pi_{\text{tr}} \rangle}{\|\Pi_{\text{tr}}\|_F^2} \right) \\ &= \frac{\text{vec}^\dagger(\Pi_{\text{tr}})}{\|\Pi_{\text{tr}}\|_F} \mathcal{T}^m \frac{\text{vec}(\Pi_{\text{tr}})}{\|\Pi_{\text{tr}}\|_F} \end{aligned} \quad (\text{A3})$$

where the twirling superchannel [18, 19, 22] is

$$\mathcal{T} = \mathbb{E}[\mathcal{G}_{\text{tr}} \otimes \tilde{\mathcal{G}}] \quad (\text{A4})$$

and $\mathcal{G}_{\text{tr}} = \mathcal{G} \Pi_{\text{tr}}$. Changing the gate-set \mathbb{G} to $\mathcal{U} \mathbb{G} \mathcal{U}^\dagger$ for some physical unitary \mathcal{U} leaves $\Pi_{\text{tr}} = \mathcal{U} \Pi_{\text{tr}} \mathcal{U}^\dagger$. Therefore

$$f_{\text{tr}}(\tilde{\mathbb{G}}, \mathcal{U} \mathbb{G} \mathcal{U}^\dagger, m) = \frac{\text{vec}^\dagger(\mathcal{U} \Pi_{\text{tr}})}{\|\Pi_{\text{tr}}\|_F} \mathcal{T}^m \frac{\text{vec}(\mathcal{U} \Pi_{\text{tr}})}{\|\Pi_{\text{tr}}\|_F} . \quad (\text{A5})$$

The spectrum of \mathcal{T} is unchanged under the basis change $\mathcal{G} \rightarrow \mathcal{U} \mathcal{G} \mathcal{U}^\dagger$. Moreover, its most important eigenvectors are as follows:

Lemma 4. *Let p be the highest eigenvalue of \mathcal{T} and*

$$\mathcal{A}_m := p^{-m} \mathbb{E} \left[(\mathcal{G}_{\text{tr},m:1})^\dagger \Pi_{\text{tr}} \tilde{\mathcal{G}}_{m:1} \right] , \quad (\text{A6a})$$

$$\mathcal{B}_m := p^{-m} \mathbb{E} \left[\tilde{\mathcal{G}}_{m:1} \Pi_{\text{tr}} (\mathcal{G}_{\text{tr},m:1})^\dagger \right] . \quad (\text{A6b})$$

Then we have

$$\text{vec}^\dagger(\mathcal{A}_\infty^T) \mathcal{T} = p \text{vec}^\dagger(\mathcal{A}_\infty^T) , \quad (\text{A7a})$$

$$\mathcal{T} \text{vec}(\mathcal{B}_\infty) = p \text{vec}(\mathcal{B}_\infty) . \quad (\text{A7b})$$

Proof. By eq. (A2),

$$\text{vec}(\mathcal{B}_m) = p^{-m} \mathbb{E} \left[(\mathcal{G}_{\text{tr},m:1})^* \otimes \tilde{\mathcal{G}}_{m:1} \right] \text{vec}(\Pi_{\text{tr}}) . \quad (\text{A8})$$

As the Liouville representation is real-valued and the \mathcal{G}_j are independent,

$$\text{vec}(\mathcal{B}_m) = (\mathcal{T}/p)^m \text{vec}(\Pi_{\text{tr}}) . \quad (\text{A9})$$

Since the noisy gate-set $\tilde{\mathbb{G}}$ is a small perturbation from \mathbb{G} the spectrum of \mathcal{T} will be slightly perturbed from $\{1, 0, 0, \dots\}$. Therefore $(\mathcal{T}/p)^m$ approaches a rank 1 projector as m increases and so $\text{vec}(\mathcal{B}_\infty)$ is a +1-eigenvector of \mathcal{T}/p .

The same argument applies to \mathcal{A}_∞^T . \square

Lemma 4 allows us to write

$$\mathcal{T} = p \frac{\text{vec}(\mathcal{B}_\infty) \text{vec}^\dagger(\mathcal{A}_\infty^T)}{\langle \mathcal{A}_\infty^T, \mathcal{B}_\infty \rangle} + \Delta , \quad (\text{A10})$$

with $\Delta \text{vec}(\mathcal{B}_\infty) = \text{vec}^\dagger(\mathcal{A}_\infty^T) \Delta = 0$. In eq. (A5), we can expand the vectors as

$$\frac{\text{vec}^\dagger(\mathcal{U} \Pi_{\text{tr}})}{\|\Pi_{\text{tr}}\|_F} = a(\mathcal{U}) \frac{\text{vec}^\dagger(\mathcal{A}_\infty^T)}{\|\mathcal{A}_\infty\|_F} + \sqrt{1 - a^2(\mathcal{U})} w^\dagger(\mathcal{U}) \quad (\text{A11a})$$

$$\frac{\text{vec}(\mathcal{U} \Pi_{\text{tr}})}{\|\Pi_{\text{tr}}\|_F} = b(\mathcal{U}) \frac{\text{vec}(\mathcal{B}_\infty)}{\|\mathcal{B}_\infty\|_F} + \sqrt{1 - b^2(\mathcal{U})} v(\mathcal{U}) \quad (\text{A11b})$$

where

$$a(\mathcal{U}) := \frac{\langle \mathcal{A}_\infty^T, \mathcal{U} \rangle}{\|\Pi_{\text{tr}}\|_F^2} \left(\frac{\|\mathcal{A}_\infty\|_F^2}{\|\Pi_{\text{tr}}\|_F^2} \right)^{-1/2} , \quad (\text{A12})$$

$$b(\mathcal{U}) := \frac{\langle \mathcal{U}, \mathcal{B}_\infty \rangle}{\|\Pi_{\text{tr}}\|_F^2} \left(\frac{\|\mathcal{B}_\infty\|_F^2}{\|\Pi_{\text{tr}}\|_F^2} \right)^{-1/2} . \quad (\text{A13})$$

and $v(\mathcal{U})$, $w(\mathcal{U})$ are implicitly defined unit vectors. Using this expansion together with eq. (A10) in eq. (A5) yields the following result:

Theorem 5 (Total gate-set circuit fidelity). *The gate-set circuit fidelity obeys*

$$\mathcal{F}(\tilde{\mathbb{G}}, \mathcal{U} \mathbb{G} \mathcal{U}^\dagger, m) = \frac{1}{d} + \frac{d-1}{d} (C(\mathcal{U}) p^m + D(m, \mathcal{U})) , \quad (\text{A14})$$

where

$$\begin{aligned} C(\mathcal{U}) &:= \frac{\langle \mathcal{A}_\infty^T, \mathcal{U} \rangle \langle \mathcal{U}, \mathcal{B}_\infty \rangle}{\|\Pi_{\text{tr}}\|_F^2 \|\Pi_{\text{tr}}\|_F^2} \left(\frac{\langle \mathcal{A}_\infty^T, \mathcal{B}_\infty \rangle}{\|\Pi_{\text{tr}}\|_F^2} \right)^{-1} \\ &= \frac{\langle \Pi_{\text{tr}}, \mathcal{A}_\infty \mathcal{U} \rangle \langle \Pi_{\text{tr}}, \mathcal{U}^\dagger \mathcal{B}_\infty \rangle}{\|\Pi_{\text{tr}}\|_F^2 \|\Pi_{\text{tr}}\|_F^2} \frac{\|\Pi_{\text{tr}}\|_F^2}{\langle \Pi_{\text{tr}}, \mathcal{A}_\infty \mathcal{B}_\infty \rangle} \end{aligned} \quad (\text{A15a})$$

$$D(m, \mathcal{U}) := \sqrt{1 - a^2(\mathcal{U})} \sqrt{1 - b^2(\mathcal{U})} w(\mathcal{U})^\dagger \Delta^m v(\mathcal{U}) . \quad (\text{A15b})$$

In [18–20] it is shown that standard RB provides an estimate of p . Notice that p is independent of the basis in which the ideal gate-set of comparison, $\mathcal{U} \mathbb{G} \mathcal{U}^\dagger$, is expressed.

From eq. (A14), it is straightforward to show that

$$\begin{aligned} \delta(m, \mathcal{U}) &:= \frac{f_{\text{tr}}(\tilde{\mathbb{G}}, \mathcal{U} \mathbb{G} \mathcal{U}^\dagger, m+1)}{f_{\text{tr}}(\tilde{\mathbb{G}}, \mathcal{U} \mathbb{G} \mathcal{U}^\dagger, m)} - p = \\ &= \frac{\sqrt{1 - a^2(\mathcal{U})} \sqrt{1 - b^2(\mathcal{U})} w(\mathcal{U})^\dagger \Delta^m (\Delta - p \Pi_{\text{tr}}) v(\mathcal{U})}{f_{\text{tr}}(\tilde{\mathbb{G}}, \mathcal{U} \mathbb{G} \mathcal{U}^\dagger, m)} , \end{aligned} \quad (\text{A16})$$

which is exponentially suppressed. We show in the next section that the eigenvalues of Δ are at most of order $\sqrt{1-p}$, which ensures a very fast decay, as shown in fig. 1. Equation (11) is in fact a reformulation of eq. (A16).

Appendix B: Varying the ideal gate-set of comparison

In this section, we prove proposition 2 by determining how the basis \mathcal{U} of the ideal gate-set $\mathcal{U}\mathbb{G}\mathcal{U}^\dagger$ affects the coefficients in eq. (A14).

Let \mathbb{G} be an ideal gate set defined with respect to the SPAM procedures. We can write the elements of a noisy gate-set as

$$\tilde{\mathcal{G}} = \mathcal{G} + \delta_{\mathcal{G}}^{(I)} \mathcal{G}, \quad (\text{B1})$$

so that the perturbations $\delta_{\mathcal{G}}$ both capture the errors in the noisy gate and the mismatch with the targeted computational basis. Under gate-independent noise with no basis mismatch, $\tilde{\mathbb{G}} = \mathcal{E}\mathbb{G}$ and the infidelity of the perturbed operations $\mathcal{I} + \delta_{\mathcal{G}}^{(I)}$ is $r(\mathcal{E}) := 1 - F(\mathcal{E}, \mathcal{I})$. A basis mismatch will change the infidelity of the perturbations roughly to $r(\mathcal{U}\mathcal{E}) + r(\mathcal{U}^\dagger)$ for some unitary channel \mathcal{U} , which will typically differ substantially from the fidelity inferred from the associated RB experiment.

Experimentally, such basis mismatches will be relatively small as operations will be somewhat consistent with SPAM procedures. Under this assumption, we now show that there exists an alternate perturbative expansion,

$$\tilde{\mathcal{G}} = \mathcal{U}\mathcal{G}\mathcal{U}^\dagger + \delta_{\mathcal{G}}^{(U)} \mathcal{U}\mathcal{G}\mathcal{U}^\dagger, \quad (\text{B2})$$

for which $r(\mathcal{I} + \mathbb{E}\delta_{\mathcal{G}}^{(U)})$ is in line with the data resulting from an RB experiment.

In appendix A, we showed that $(\mathcal{T}/p)^n$ converges to a rank-1 projector. We now quantify the rate of convergence. Recall that \mathcal{T} is perturbed from a rank-1 projector with spectrum $\{1, 0, 0, \dots\}$. Hence, by the Bauer-Fike theorem [23], for any eigenvalue $\lambda \neq p$ of \mathcal{T} ,

$$\begin{aligned} |\lambda - 0| &\leq \|\mathbb{E}[\mathcal{G}_{\text{tr}} \otimes \delta_{\mathcal{G}}^{(I)} \mathcal{G}]\|_2 && (\text{Bauer-Fike}) \\ &\leq \mathbb{E}\|\mathcal{G}_{\text{tr}} \otimes \delta_{\mathcal{G}}^{(I)} \mathcal{G}\|_2 && (\text{triangle ineq.}) \\ &= \mathbb{E}\|\delta_{\mathcal{G}}^{(I)}\|_2 && (\text{Unitary invariance}) \\ &\leq O\left(\mathbb{E}\sqrt{r(\mathcal{I} + \delta_{\mathcal{G}}^{(I)})}\right) && ([24]) \\ &\leq O\left(\sqrt{r(\mathcal{I} + \mathbb{E}\delta_{\mathcal{G}}^{(I)})}\right) && (\text{concavity}) \end{aligned}$$

This spectral profile implies that $(\mathcal{T}/p)^n$ converges quickly to a rank-1 operator since the eigenvalues close to zero are exponentially suppressed.

Hence, we can approximate the asymptotic eigen-operators defined in eqs. (A6a) and (A6b) as:

$$\mathcal{A}_\infty = \mathcal{A}_4 + O(r(\mathcal{I} + \mathbb{E}\delta_{\mathcal{G}}^{(I)})^2), \quad (\text{B3a})$$

$$\mathcal{B}_\infty = \mathcal{B}_4 + O(r(\mathcal{I} + \mathbb{E}\delta_{\mathcal{G}}^{(I)})^2). \quad (\text{B3b})$$

In the simple noise model $\mathcal{E}_L\mathbb{G}\mathcal{E}_R$, $\mathcal{A}_\infty \propto \Pi_{\text{tr}}\mathcal{E}_R$ and $\mathcal{B}_\infty \propto \mathcal{E}_L\Pi_{\text{tr}}$. To pursue the analogy, we denote the m^{th} order right and left errors as

$$\mathcal{E}_R^{(m)} = \mathbb{E}\left[(\mathcal{G}_{m:1})^\dagger \tilde{\mathcal{G}}_{m:1}\right], \quad (\text{B4a})$$

$$\mathcal{E}_L^{(m)} = \mathbb{E}\left[\tilde{\mathcal{G}}_{m:1}(\mathcal{G}_{m:1})^\dagger\right]. \quad (\text{B4b})$$

Combining eq. (B4) and eq. (B3), we get

$$\mathcal{A}_\infty \propto \Pi_{\text{tr}}\mathcal{E}_R^{(4)} + O(r(\mathcal{I} + \mathbb{E}\delta_{\mathcal{G}}^{(I)})^2), \quad (\text{B5a})$$

$$\mathcal{B}_\infty \propto \mathcal{E}_L^{(4)}\Pi_{\text{tr}} + O(r(\mathcal{I} + \mathbb{E}\delta_{\mathcal{G}}^{(I)})^2). \quad (\text{B5b})$$

The structure of single-qubit error channels allows us to pursue a deeper analysis. It follows from the channel analysis provided in [25] that, for high-fidelity qubit-channels, the 3×3 submatrix acting on the traceless hyperplane can always be decomposed as

$$\mathcal{E}\Pi_{\text{tr}} = \mathcal{D}\mathcal{V}\Pi_{\text{tr}} \quad (\text{B6})$$

where \mathcal{V} is a physical unitary, and \mathcal{D} is an incoherent process. Here we label a channel \mathcal{D} incoherent if

$$\frac{\langle \Pi_{\text{tr}}, \mathcal{D} \rangle}{\|\Pi_{\text{tr}}\|_F^2} = \frac{\|\mathcal{D}\Pi_{\text{tr}}\|_F}{\|\Pi_{\text{tr}}\|_F} + O(r(\mathcal{D})^2). \quad (\text{B7})$$

Incoherent channels have the additional property that , given an error channel Λ [26]

$$\frac{\langle \Pi_{\text{tr}}, \mathcal{D}\Lambda \rangle}{\|\Pi_{\text{tr}}\|_F^2} = \frac{\langle \Pi_{\text{tr}}, \mathcal{D} \rangle}{\|\Pi_{\text{tr}}\|_F^2} \frac{\langle \Pi_{\text{tr}}, \Lambda \rangle}{\|\Pi_{\text{tr}}\|_F^2} + O(r(\mathcal{D}\Lambda)^2). \quad (\text{B8})$$

Expressing the 4th order right error $\mathcal{E}_R^{(4)}$ as

$$\mathcal{E}_R^{(4)}\Pi_{\text{tr}} = \mathcal{D}\mathcal{V}\Pi_{\text{tr}}. \quad (\text{B9})$$

allows us to maximally correct it through a physical unitary:

$$F(\mathcal{E}_R^{(4)}\mathcal{V}^\dagger, \mathcal{I}) = \max_{\mathcal{U}} F(\mathcal{E}_R^{(4)}\mathcal{U}, \mathcal{I}) \geq F(\mathcal{E}_R^{(4)}, \mathcal{I}). \quad (\text{B10})$$

Using the property expressed in eq. (B8), we get:

$$\frac{\langle \Pi_{\text{tr}}, \mathcal{E}_R^{(4)}\mathcal{V}^\dagger\mathcal{V}\mathcal{E}_L^{(4)} \rangle}{\|\Pi_{\text{tr}}\|_F} = \frac{\langle \Pi_{\text{tr}}, \mathcal{E}_R^{(4)}\mathcal{V}^\dagger \rangle}{\|\Pi_{\text{tr}}\|_F} \frac{\langle \Pi_{\text{tr}}, \mathcal{V}\mathcal{E}_L^{(4)} \rangle}{\|\Pi_{\text{tr}}\|_F} + O(r(\mathcal{I} + \mathbb{E}\delta_{\mathcal{G}}^{(I)})^2). \quad (\text{B11})$$

Looking back at theorem 5 and using eqs. (B11), (B5a) and (B5b) results in

$$C(\mathcal{V}^\dagger) = 1 + O\left(r(\mathcal{I} + \mathbb{E}\delta_{\mathcal{G}}^{(I)})^2\right). \quad (\text{B12})$$

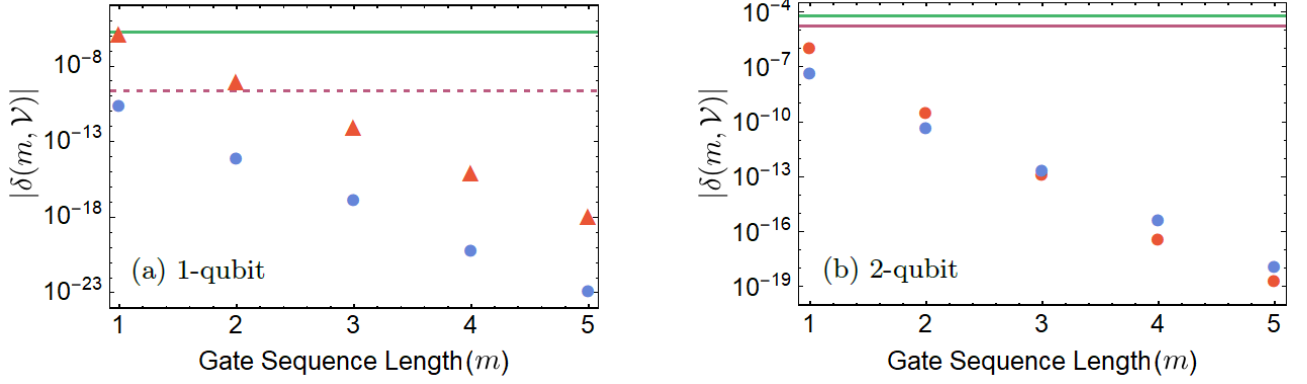


FIG. 1: Absolute value of the deviation $\delta(m, \mathcal{V})$, described in eq. (11) (also see eq. (A16)), as function of circuit length m with noise model generated by $\tilde{\mathcal{G}}_x = \mathcal{P}(\sigma_z, 10^{-1})\mathcal{G}_x$ and $\tilde{\mathcal{G}}_y = \mathcal{P}(\sigma_z, 10^{-1})\mathcal{G}_y$, $\tilde{\mathcal{G}}_{CZ} = \mathcal{P}(\sigma_z^1\sigma_z^2 - \sigma_z^1 - \sigma_z^2, \pi/2 + 10^{-1})$ (see eq. (18)). The red triangles are obtained with the choice of basis $\mathcal{V} = \mathcal{I}$, while the blue circles are obtained with the choice $\mathcal{V} = \mathcal{U}$ where \mathcal{U} is found through eq. (17). The purple horizontal dashed line corresponds to $(1-p)^2$, while the full green line corresponds to $(1 - \mathcal{F}(\tilde{\mathcal{G}}, \mathbb{G}, 1))^2$. For both ideal gate-sets \mathbb{G} and $\mathcal{U}\mathbb{G}\mathcal{U}^\dagger$, the deviation becomes quickly negligible as the sequence length increases. In fact, in the case $\mathcal{V} = \mathcal{U}$ (blue circles), the deviation is always below $(1-p)^2$.

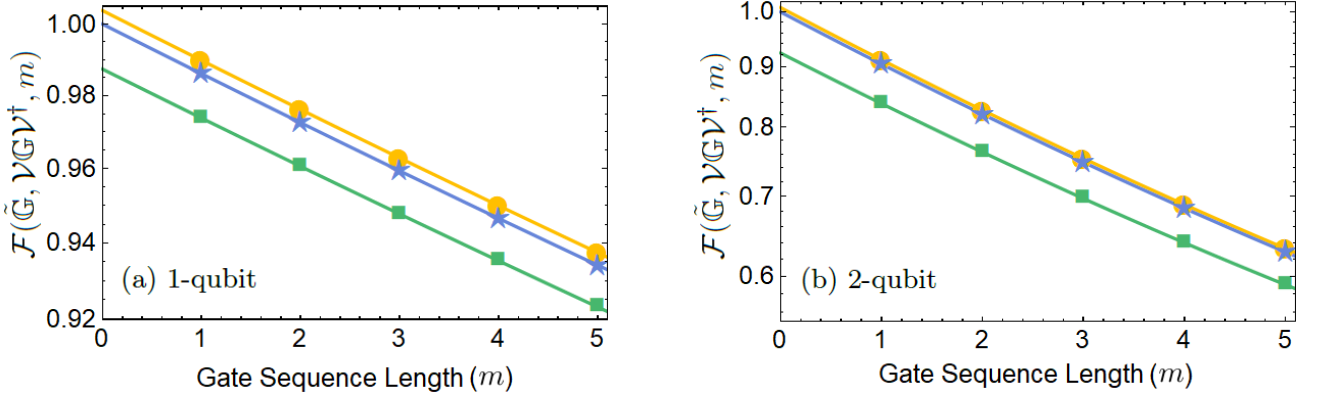


FIG. 2: gate-set circuit fidelity $\mathcal{F}(\tilde{\mathcal{G}}, \mathcal{V}\mathbb{G}\mathcal{V}^\dagger, m)$ as a function of circuit length m with noise model generated by $\tilde{\mathcal{G}}_x = \mathcal{P}(\sigma_x, \pi/2 + 10^{-1})$, $\tilde{\mathcal{G}}_y = \mathcal{P}(\sigma_y, \pi/2 + 10^{-1})$, $\tilde{\mathcal{G}}_{CZ} = \mathcal{P}(\sigma_z^1\sigma_z^2 - \sigma_z^1 - \sigma_z^2, \pi/2 + 10^{-1})$ (see eq. (18)). The different colors portray choices of basis; the yellow circles $\mathcal{V} = \mathcal{I}$, the blue stars $\mathcal{V} = \mathcal{U}$ where \mathcal{U} is found through eq. (17), and the green squares $\mathcal{V} = \mathcal{U}^2$. Here the lines correspond to the fit for sequence lengths of $m=5$ to 10. The choice $\mathcal{V} = \mathcal{U}$ produces the evolution prescribed by proposition 2, which through extrapolation has an intercept of 1.

Since both \mathcal{V} and $\mathcal{E}_L^{(4)}$ have at most infidelity of order $r(\mathcal{I} + \mathbb{E}\delta_{\mathcal{G}}^{(I)})$, it follows that the composition $\mathcal{V}\mathcal{E}_L^{(4)}$ must also have an infidelity of order $r(\mathcal{I} + \mathbb{E}\delta_{\mathcal{G}}^{(I)})$, which guarantees

$$\sqrt{1 - b^2(\mathcal{V}^\dagger)} = O\left(\sqrt{r(\mathcal{I} + \mathbb{E}\delta_{\mathcal{G}}^{(I)})}\right), \quad (\text{B13})$$

while incoherence guarantees

$$\sqrt{1 - a^2(\mathcal{V}^\dagger)} = O\left(r(\mathcal{I} + \mathbb{E}\delta_{\mathcal{G}}^{(I)})\right). \quad (\text{B14})$$

Using

$$|w(\mathcal{V}^\dagger)^\dagger \Delta v(\mathcal{V}^\dagger)| \leq \mathbb{E}\|\delta_{\mathcal{G}}^{(I)}\|_2 \leq O\left(\sqrt{r(\mathcal{I} + \mathbb{E}\delta_{\mathcal{G}}^{(I)})}\right) \quad (\text{B15})$$

in eq. (A15b), we find

$$D(1, \mathcal{V}^\dagger) = O\left(r(\mathcal{I} + \mathbb{E}\delta_{\mathcal{G}}^{(I)})^2\right), \quad (\text{B16})$$

which, together with eqs. (A14) and (B12) leads to

$$f_{\text{tr}}(\tilde{\mathcal{G}}, \mathcal{V}^\dagger\mathbb{G}\mathcal{V}, m) = p^m + O\left(r(\mathcal{I} + \mathbb{E}\delta_{\mathcal{G}}^{(I)})^2\right). \quad (\text{B17})$$

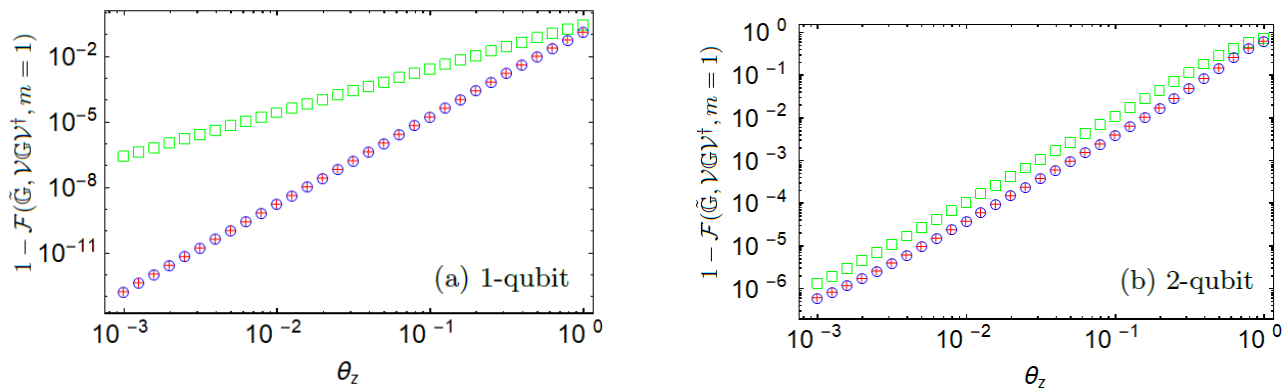


FIG. 3: $1 - \mathcal{F}(\tilde{\mathcal{G}}, \mathcal{V}\mathcal{G}\mathcal{V}^\dagger, m=1)$ as function of the angle θ_z in noise model generated by $\tilde{\mathcal{G}}_x = \mathcal{P}(\sigma_z, \theta_z)\mathcal{G}_x$ and $\tilde{\mathcal{G}}_y = \mathcal{P}(\sigma_z, \theta_z)\mathcal{G}_y$, $\tilde{\mathcal{G}}_{CZ} = \mathcal{P}(\sigma_z^1\sigma_z^2 - \sigma_z^1 - \sigma_z^2, \pi/2 + 10^{-1})$ (see eq. (18)), with $\mathcal{V} = \mathcal{I}$ (green squares) and $\mathcal{V} = \mathcal{U}$ (blue circles) where \mathcal{U} is found through eq. (17). The red crosses correspond to $(1-p)/2$ obtained through RB experiments.

This expression allows us to pick a better perturbative expansion than eq. (B1). Indeed, choosing

$$\tilde{\mathcal{G}} = \mathcal{V}^\dagger \mathcal{G} \mathcal{V} + \delta_{\mathcal{G}}^{(V^\dagger)} \mathcal{V}^\dagger \mathcal{G} \mathcal{V}, \quad (\text{B18})$$

ensures that the noisy operations $\mathcal{I} + \delta_{\mathcal{G}}^{(V^\dagger)}$ have an gate-set circuit infidelity which is more in line with the RB data:

$$r(\mathcal{I} + \delta_{\mathcal{G}}^{(V^\dagger)}) = \frac{d-1}{d}(1-p) + O(r(\mathcal{I} + \delta_{\mathcal{G}}^{(I)})^2). \quad (\text{B19})$$

Iterating the analysis leads to

$$f_{\text{tr}}(\tilde{\mathcal{G}}, \mathcal{V}^\dagger \mathcal{G} \mathcal{V}, m) = p^m + O((1-p)^2). \quad (\text{B20})$$

This completes the demonstration of proposition 2.

Our current proof technique relies on the structure of single-qubit channels. For higher dimensions, we conjecture that an analog of proposition 2 holds, although the scaling with the dimension is unclear.

Conjecture 6. If the fidelity of $\mathcal{E}_R^{(4)}$ is high, then \exists a physical unitary \mathcal{V}^\dagger s.t. $\mathcal{E}_R^{(4)}\mathcal{V}^\dagger$ is incoherent.

As we now show constructively, conjecture 6 holds for physically motivated noise models composed of gener-

alized dephasing, amplitude damping, and unitary processes. Under such noise models,

$$\mathcal{E}_R^{(4)} = \mathcal{U}_T \mathcal{D}_T \cdots \mathcal{U}_2 \mathcal{D}_2 \mathcal{U}_1 \mathcal{D}_1 \quad (\text{B21})$$

for some unitaries \mathcal{U}_i and incoherent channels \mathcal{D}_i .

The channel $\mathcal{U}\mathcal{D}\mathcal{U}^\dagger$ is incoherent for any physical unitary \mathcal{U} , and the composition of incoherent channels is also incoherent, so eq. (B21) can be rewritten as $\mathcal{E}_R^{(4)} = \mathcal{D}\mathcal{V}$, where \mathcal{D} and \mathcal{V} are incoherent and unitary respectively:

$$\mathcal{D} = (\mathcal{U}_T \mathcal{D}_T \mathcal{U}_T^\dagger) \cdots (\mathcal{U}_{T:1} \mathcal{D}_1 \mathcal{U}_{T:1}^\dagger) \quad (\text{B22})$$

$$\mathcal{V} = \mathcal{U}_{T:1}. \quad (\text{B23})$$

ACKNOWLEDGMENTS

The authors acknowledge helpful discussions with Timothy J. Proctor and Hui Khoon Ng. This research was supported by the U.S. Army Research Office through grant W911NF-14-1-0103. This research was undertaken thanks in part to funding from TQT, CIFAR, the Government of Ontario, and the Government of Canada through CFREF, NSERC and Industry Canada.

[1] J. Emerson, R. Alicki, and K. Życzkowski, *Journal of Optics B: Quantum and Semiclassical Optics* **7**, S347 (2005).
 [2] B. Levi, C. C. Lopez, J. Emerson, and D. G. Cory, *Physical Review A* **75**, 022314 (2007).
 [3] E. Knill, D. Leibfried, R. Reichle, J. Britton, R. Blakestad, J. D. Jost, C. Langer, R. Ozeri, S. Seidelin, and D. J. Wineland, *Physical Review A* **77**, 012307 (2008).

[4] C. Dankert, R. Cleve, J. Emerson, and E. Livine, *Physical Review A* **80**, 012304 (2009).
 [5] E. Magesan, J. M. Gambetta, and J. Emerson, *Physical Review Letters* **106**, 180504 (2011).
 [6] E. Magesan, J. M. Gambetta, and J. Emerson, *Physical Review A* **85**, 042311 (2012).
 [7] A. Dugas, J. J. Wallman, and J. Emerson, *Physical Review A* **92**, 060302 (2015), arXiv:1508.06312 [quant-ph].

- [8] A. W. Cross, E. Magesan, L. S. Bishop, J. A. Smolin, and J. M. Gambetta, *npj Quantum Information* **2**, 16012 (2016), arXiv:1510.02720 [quant-ph].
- [9] J. P. Gaebler, A. M. Meier, T. R. Tan, R. Bowler, Y. Lin, D. Hanneke, J. D. Jost, J. P. Home, E. Knill, D. Leibfried, and D. J. Wineland, *Physical Review Letters* **108**, 260503 (2012).
- [10] A. D. Córcoles, J. M. Gambetta, J. M. Chow, J. A. Smolin, M. Ware, J. Strand, B. L. T. Plourde, and M. Steffen, *Physical Review A* **87**, 030301 (2013).
- [11] J. Kelly, R. Barends, B. Campbell, Y. Chen, Z. Chen, B. Chiaro, A. Dunsworth, A. G. Fowler, I.-C. Hoi, E. Jeffrey, A. Megrant, J. Mutus, C. Neill, P. J. J. O'Malley, C. Quintana, P. Roushan, D. Sank, A. Vainsencher, J. Wenner, T. C. White, A. N. Cleland, and J. M. Martinis, *Physical Review Letters* **112**, 240504 (2014).
- [12] R. Barends, J. Kelly, A. Megrant, A. Veitia, D. Sank, E. Jeffrey, T. C. White, J. Mutus, A. G. Fowler, B. Campbell, Y. Chen, Z. Chen, B. Chiaro, A. Dunsworth, C. Neill, P. O'Malley, P. Roushan, A. Vainsencher, J. Wenner, A. N. Korotkov, A. N. Cleland, and J. M. Martinis, *Nature* **508**, 500 (2014), letter.
- [13] L. Casparis, T. W. Larsen, M. S. Olsen, F. Kuemmeth, P. Krogstrup, J. Nygård, K. D. Petersson, and C. M. Marcus, *Physical Review Letters* **116**, 150505 (2016), arXiv:1512.09195 [cond-mat.mes-hall].
- [14] M. Takita, A. D. Córcoles, E. Magesan, B. Abdo, M. Brink, A. Cross, J. M. Chow, and J. M. Gambetta, *Physical Review Letters* **117**, 210505 (2016), arXiv:1605.01351 [quant-ph].
- [15] S. Sheldon, E. Magesan, J. M. Chow, and J. M. Gambetta, *Phys. Rev. A* **93**, 060302 (2016), arXiv:1603.04821 [quant-ph].
- [16] D. C. McKay, S. Filipp, A. Mezzacapo, E. Magesan, J. M. Chow, and J. M. Gambetta, *Physical Review Applied* **6**, 064007 (2016), arXiv:1604.03076 [quant-ph].
- [17] D. C. McKay, S. Sheldon, J. A. Smolin, J. M. Chow, and J. M. Gambetta, *ArXiv e-prints* (2017), arXiv:1712.06550 [quant-ph].
- [18] T. Proctor, K. Rudinger, K. Young, M. Sarovar, and R. Blume-Kohout, *Physical Review Letters* **119**, 130502 (2017), arXiv:1702.01853 [quant-ph].
- [19] J. J. Wallman, *Quantum* **2**, 47 (2018).
- [20] S. T. Merkel, E. J. Pritchett, and B. H. Fong, *ArXiv e-prints* (2018), arXiv:1804.05951 [quant-ph].
- [21] J. Qi and H. Khoon Ng, *ArXiv e-prints* (2018), arXiv:1805.10622 [quant-ph].
- [22] T. Chasseur and F. K. Wilhelm, *Physical Review A - Atomic, Molecular, and Optical Physics* **92**, 042333 (2015), arXiv:1505.00580v2.
- [23] F. L. Bauer and C. T. Fike, *Numerische Mathematik* **2**, 137 (1960).
- [24] J. J. Wallman, *ArXiv e-prints* (2015), arXiv:1511.00727 [quant-ph].
- [25] M. B. Ruskai, S. Szarek, and E. Werner, *Linear Algebra and its Applications* **347**, 159 (2002).
- [26] A. C. Dugas, J. J. Wallman, and J. Emerson, *ArXiv e-prints* (2016), arXiv:1610.05296 [quant-ph].